

## LINKING GAS FRACTIONS TO BIMODALITIES IN GALAXY PROPERTIES

SHEILA J. KANNAPPAN<sup>1</sup>

## ABSTRACT

As an extension of known correlations, galaxies over four decades in stellar mass are shown to obey a strong correlation between  $u - K$  colors and gas-to-stellar mass (G/S) ratios, using neutral H I gas masses and stellar mass-to-light ratios derived from optical colors. The correlation holds for G/S ratios ranging from nearly 10:1 to 1:100 for a sample obtained by merging the SDSS DR2, 2MASS, and HYPERLEDA H I catalogs. This result implies that  $u - K$  colors can be calibrated to provide “photometric gas fractions” for statistical applications. In this paper this technique is applied to a sample of  $\sim 35,000$  SDSS-2MASS galaxies to examine the relationship of gas fractions to observed bimodalities in galaxy properties as a function of stellar mass and optical color. The recently identified transition in galaxy properties at stellar masses  $\sim 2-3 \times 10^{10} M_{\odot}$  corresponds to a shift in gas richness, which divides low-mass late-type galaxies with G/S  $\sim 1:1$  from high-mass galaxies with intermediate to low gas fractions. Early-type galaxies below the transition mass also show elevated gas fractions, consistent with formation scenarios involving mergers of low-mass gas-rich systems and/or cold-mode gas accretion.

*Subject headings:* galaxies: evolution

## 1. INTRODUCTION

Analyses of galaxies in the Sloan Digital Sky Survey (SDSS) have demonstrated two distinct bimodalities in galaxy properties: a bimodality between recent-burst dominated and more continuous star formation histories (SFHs) as a function of stellar mass  $M_*$ , divided at  $M_* \sim 3 \times 10^{10} M_{\odot}$  (Kauffmann et al. 2003b), and a bimodality between blue late-type and red early-type galaxy sequences as a function of optical color, divided at  $u - r \sim 2.2$  (Strateva et al. 2001; Hogg et al. 2002; Blanton et al. 2003b). Recently, Baldry et al. (2004) have partially unified these observations, demonstrating a color transition within each of the two galaxy sequences at  $M_* \sim 2 \times 10^{10} M_{\odot}$ , as well as an increase in the relative number density of red sequence galaxies above  $\sim 2-5 \times 10^{10} M_{\odot}$ . They also argue that the number density of the red sequence is consistent with a major-merger origin. However, the cause of the color and SFH transitions at  $\sim 2-3 \times 10^{10} M_{\odot}$  remains to be explained.

Several physical processes that influence SFHs may imprint a transition mass on the galaxy population. Supernova-driven gas blowout will preferentially affect halos with small escape velocities (Dekel & Silk 1986), although simulations suggest that the mass threshold for blowout may be closer to  $10^7 M_{\odot}$  than to  $10^{10} M_{\odot}$  (Mac Low & Ferrara 1999). Cold-mode gas accretion may dominate in low-mass halos whose gas fails to shock to the virial temperature (Birnboim & Dekel 2003; Katz et al. 2003); here analytic estimates give a threshold mass of a few times  $10^{11} M_{\odot}$  including dark matter, so a link to the observed transition at  $M_* \sim 2-3 \times 10^{10} M_{\odot}$  is plausible. Finally, observations suggest that inefficient star formation may be typical of disk-dominated galaxies with  $V_c \lesssim 120 \text{ km s}^{-1}$ , possibly reflecting the relative importance of supernova feedback as opposed to other turbulence drivers in supporting the interstellar medium against gravitational instability (Dalcanton et al. 2004).

All of these processes involve gas – its expulsion, accretion, or rate of consumption. Thus examining how the gas properties of galaxies vary with color and stellar mass may offer vital clues to the origin of the transition mass and the color shifts within the red and blue sequences. Unfortunately, tracing the dominant

neutral phase of the interstellar medium requires H I 21-cm line observations, which are challenging even at the modest redshifts probed by the SDSS. To make full use of the statistical power of the SDSS, an alternate strategy is required.

Building on earlier optical work (e.g., Roberts 1969), Bothun (1984) has demonstrated a remarkably tight correlation between H I mass to  $H$ -band luminosity ratios and  $B - H$  colors. Going one step further, the present work describes a method for estimating gas-to-stellar mass ratios using  $u - K$  colors obtained from the SDSS and Two Micron All Sky Survey (2MASS) databases. This “photometric gas fraction” technique is calibrated using H I data from the recently expanded HYPERLEDA H I catalog. When the technique is applied to a sample of  $\sim 35,000$  SDSS-2MASS galaxies at  $z < 0.1$ , the transition mass of  $2-3 \times 10^{10} M_{\odot}$  is observed to correspond to a shift in gas richness found separately in both galaxy color sequences. This result implies that any explanation of the transition mass via gas physics must directly or indirectly affect the gas in low-mass early-type galaxies as well as dwarf late-type systems.

## 2. DATA

Optical, near-IR, and H I data were obtained from the SDSS second data release (DR2, Abazajian et al. 2004), the 2MASS all-sky extended source catalog (XSC, Jarrett et al. 2000), and the HYPERLEDA homogenized H I catalog (Paturel et al. 2003). Merged catalogs were constructed containing all  $z < 0.1$ ,  $r < 17.77$ ,  $K < 15$  galaxies with positions matched to within  $6''$  and with reliable redshifts and magnitudes based on data flags and catalogued errors (magnitude errors  $< 0.3$  in  $K$ ,  $< 0.4$  in H I, and  $< 0.15$  in  $ugr$ ). The 2MASS magnitude limit was set fainter than the completeness limit to improve statistics on dwarf and low surface brightness galaxies. As the 2MASS XSC has uneven depth, it probes significantly fainter than the completeness limit in some areas of the sky. Because of their marginal detectability, galaxies with measured gas-to-stellar mass ratios greater than two were targeted for individual inspection, and eight were rejected as having unreliable 2MASS or SDSS pipeline reductions. These rejections exacerbate the shortage of IR-faint galaxies. The final samples are: SDSS-HYPERLEDA

<sup>1</sup> Harlan Smith Fellow, McDonald Observatory, The University of Texas at Austin, 1 University Station C1402, Austin, TX 78712-0259; sheila@astro.as.utexas.edu

(575 galaxies), SDSS-2MASS-HYPERLEDA (346 galaxies), and SDSS-2MASS (35,166 galaxies). An additional requirement for the SDSS-2MASS sample was that the Local Group motion-corrected redshift be greater than 1000 km s<sup>-1</sup>.

All optical and IR magnitudes used here are fitted magnitudes, i.e. SDSS model magnitudes and 2MASS extrapolated total magnitudes. The SDSS magnitudes are corrected for Galactic extinction using the DR2 tabulated values and k-corrected to redshift zero using **kcorrect v3.2** (Blanton et al. 2003a), while the 2MASS *K*-band magnitudes are k-corrected using  $k(z) = -2.1z$  (Bell et al. 2003). Distances are computed in the concordance cosmology  $\Omega_m = 0.3$ ,  $\Omega_\Lambda = 0.7$ ,  $H_0 = 70$  km s<sup>-1</sup> Mpc<sup>-1</sup>.

### 3. RESULTS

Fig. 1a shows the basic correlation between *u*-band and 21-cm apparent magnitudes  $m_u$  and  $m_{\text{HI}}$  for the SDSS-HYPERLEDA sample. Its existence is not surprising: *u*-band light is a tracer of young massive stars, and the birth rate of young stars is known to depend on the available gas reservoir (as in the “global Schmidt law” relating the overall gas surface density and disk-averaged star formation rate, Kennicutt 1989). Most of the scatter in the  $m_u$ – $m_{\text{HI}}$  relation is not explained by the errors. This scatter likely represents variations in *u*-band extinction, molecular-to-atomic gas ratios, and the physical conditions required to convert a gas reservoir into young stars. Even without calibrating these factors, the  $m_u$ – $m_{\text{HI}}$  relation is sufficiently tight for the present application. In fact, it is tighter than one might have naively expected, perhaps indicating that even as gas content influences the star formation rate, the presence of young massive stars may influence the amount of H I detected (e.g., Shaya & Federman 1987).

Figs. 1b and 1c plot gas-to-stellar mass (G/S) ratios against *u*–*r* and *u*–*K* colors for the SDSS-2MASS-HYPERLEDA sample. Gas masses are derived from H I fluxes with a helium correction factor of 1.4, and stellar masses are derived from *K*-band fluxes using stellar mass-to-light (M/L) ratios estimated from *g*–*r* colors as in Bell et al. (2003). The resulting correlations are distance-independent and extremely strong, with Spearman rank correlation coefficients of 0.75 and 0.69, for *u*–*K* and *u*–*r* respectively. Note that the calibration sample spans the color–stellar mass relation (Fig. 2a). The strength of the *u*–*K* color–G/S relation derives both from the underlying  $m_u$ – $m_{\text{HI}}$  relation and from the close correspondence between *K*-band light and stellar mass. The latter correspondence is assumed within this work and may not apply to all starbursting systems (Pérez-González et al. 2003); however, Kauffmann et al. (2003a) find that spectroscopically determined M/L ratios generally agree well with color-based M/L ratios, even in the low-mass regime where starbursts are common.

The large dynamic range of the *u*–*K* color–G/S relation makes the relation forgiving of errors and thus well-suited to low-precision estimation of photometric gas fractions. The 0.37 dex scatter in the relation provides a basis for error estimation. Furthermore, galaxies of low and high mass define broadly similar *u*–*K* color–G/S relations in their regime of overlap (triangles and dots in Fig. 1c). It should be borne in mind that the generality of the photometric gas fraction technique as currently formulated relies on the fact that heavily dust-enshrouded star formation, as in luminous infrared galaxies, is rare in the low-*z* universe (Sanders & Mirabel 1996). In dusty systems one might find high G/S linked to *red* *u*–*K* colors. Also, the calibration given here will underestimate G/S ratios if stellar M/L ratios are

much lower than assumed and/or molecular gas corrections are large (a controversial topic; see Casoli et al. 1998; Boselli et al. 2002). The stellar M/L ratios used here are roughly consistent with maximum disk assumptions for spiral galaxies (Bell et al. 2003). Within the *ugriz* magnitude set, the best alternative to the *u*–*K* color–G/S relation is the *u*–*r* color–G/S relation. Its larger scatter may in part reflect the fact that *K*-band magnitude errors will move points along the *u*–*K* color–G/S relation, but away from the *u*–*r* color–G/S relation. However, the effect from cataloged errors is quite small (arrows in Figs. 1b and 1c), so the greater *u*–*r* scatter seems to be mostly physical.

Fig. 2a plots *u*–*r* color vs. stellar mass  $M_*$  for the  $\sim 35,000$ -galaxy SDSS-2MASS sample, with points color-coded to indicate photometric gas fractions as in Fig. 1c. The red sequence (a tight, nearly horizontal locus) and the blue sequence (a broad, curving locus with a nearly horizontal tail at low  $M_*$ ) are both evident. Within each sequence, the color-coding reveals a shift in gas fractions near a threshold mass of  $M_*^t \sim 1\text{--}3 \times 10^{10} \text{ M}_\odot$ . Massive red-sequence galaxies are extremely gas-poor (G/S as low as 1:100), whereas for red-sequence galaxies below  $M_*^t$ , intermediate gas fractions (G/S  $\sim 1:10$ ) are the norm. Likewise, massive blue-sequence galaxies have intermediate gas fractions (G/S  $\sim 1:10$ ), but blue-sequence galaxies below  $M_*^t$  are typically gas rich (G/S  $\sim 1:1$ ).

These results are shown in binned form in Fig. 2b, where the contours show the conditional probability distribution of *u*–*r* on  $M_*$ . In this plot, a vertical slice through the contours at a given mass gives the one-dimensional probability distribution for *u*–*r* colors at that mass. The conditional probability distribution is formed by weighting each galaxy by  $1/V_{\text{max}}$ , where  $V_{\text{max}}$  is the maximum volume within which it could have been detected, and then normalizing the counts in each color×mass bin by the total counts in each mass column. Bins with fewer than 4 galaxies are not considered. This algorithm is most robustly applied to truly magnitude-limited samples, but the results shown here look qualitatively similar to those of Baldry et al. (2004) for a magnitude-limited SDSS sample. Each galaxy is assigned the smallest of three  $V_{\text{max}}$  estimates, based on (i) the magnitude limit in *r*, (ii) the magnitude limit in *K*, and (iii) the distance limit imposed by the  $z < 0.1$  selection requirement.

The colored symbols in Fig. 2b show the photometric gas fraction and concentration index for each bin. Each symbol is plotted in three colors to indicate the  $\pm 1\sigma$  range of possible mean photometric gas fractions given the propagated scatter in the *u*–*K* color–G/S relation. Ovals and S-shapes identify early and late types, respectively, based on the concentration index  $C_r$  (defined as  $r_{90}/r_{50}$ , where  $r_{90}$  and  $r_{50}$  are the 90% and 50% Petrosian radii). A value of  $C_r = 2.6$  is commonly used to divide early-type and late-type morphologies when true morphological type information is lacking (Strateva et al. 2001; Kauffmann et al. 2003a; Bell et al. 2003). Fig. 2b indicates transitional values ( $2.55 < C_r < 2.65$ ) with both type symbols. Some of the bluest low-mass galaxies show transitional types, which will not be examined here. More generally, the blue sequence forms a broad strip with low concentration index, with a shift in gas richness at  $M_*^t \sim 1\text{--}3 \times 10^{10} \text{ M}_\odot$ .

Perhaps most intriguing is the coordinated shift in gas richness and concentration index within the red sequence below  $M_*^t$ . The increased gas content of the low-mass red sequence actually causes the red and blue sequences to fuse (nearly) in a plot of photometric gas fraction (*u*–*K*) vs. stellar mass (Fig. 2c). The S-shaped contours of the resulting conditional probability dis-

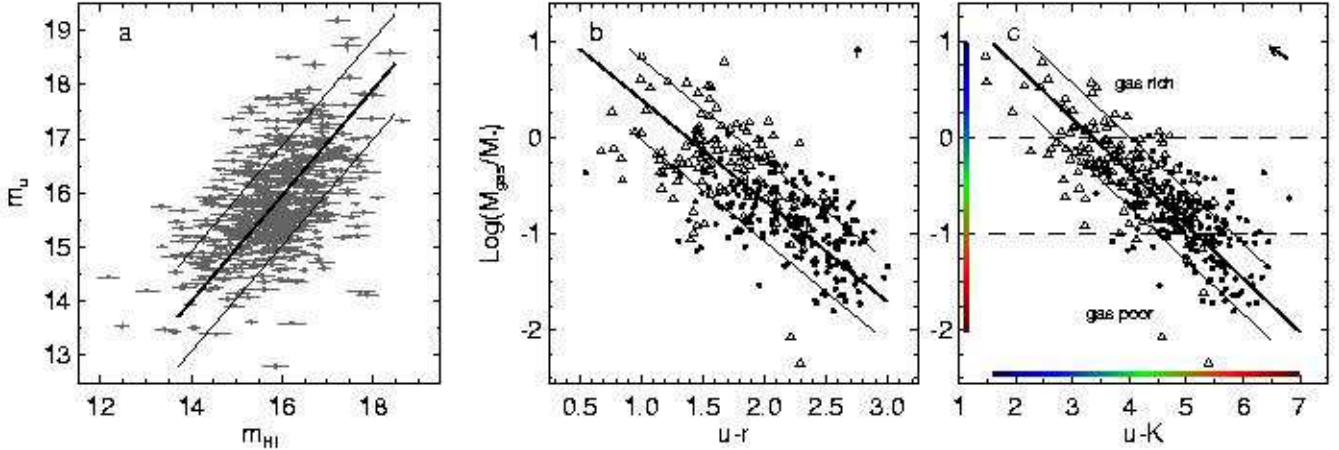


FIG. 1.— (a) Apparent  $u$ -band magnitude vs. apparent  $\mathrm{H}\alpha$  magnitude for the SDSS-HYPERLEDA sample. A bisector fit yields  $m_u = 0.33 + 0.98m_{\mathrm{HI}}$  (thick line) with  $\sigma = 0.92$  mag (thin lines). (b and c) Gas-to-stellar mass ratio vs.  $u-r$  and  $u-K$  color for the SDSS-2MASS-HYPERLEDA sample. Bisector fits yield  $\log(M_{\mathrm{gas}}/M_*) = 1.46 - 1.06(u-r)$  and  $\log(M_{\mathrm{gas}}/M_*) = 1.87 - 0.56(u-K)$  (thick lines) with  $\sigma = 0.42$  dex and 0.37 dex, respectively (thin lines). Arrows indicate the effect of a 0.3 mag error in  $K$  (the maximum allowed by selection). The color scale in panel c provides a key to the photometric gas fractions in Fig. 2. Horizontal lines demarcate gas-rich, intermediate, and gas-poor regimes. Dots and triangles mark galaxies with  $M_*$  above and below  $2 \times 10^{10} M_\odot$ , respectively.

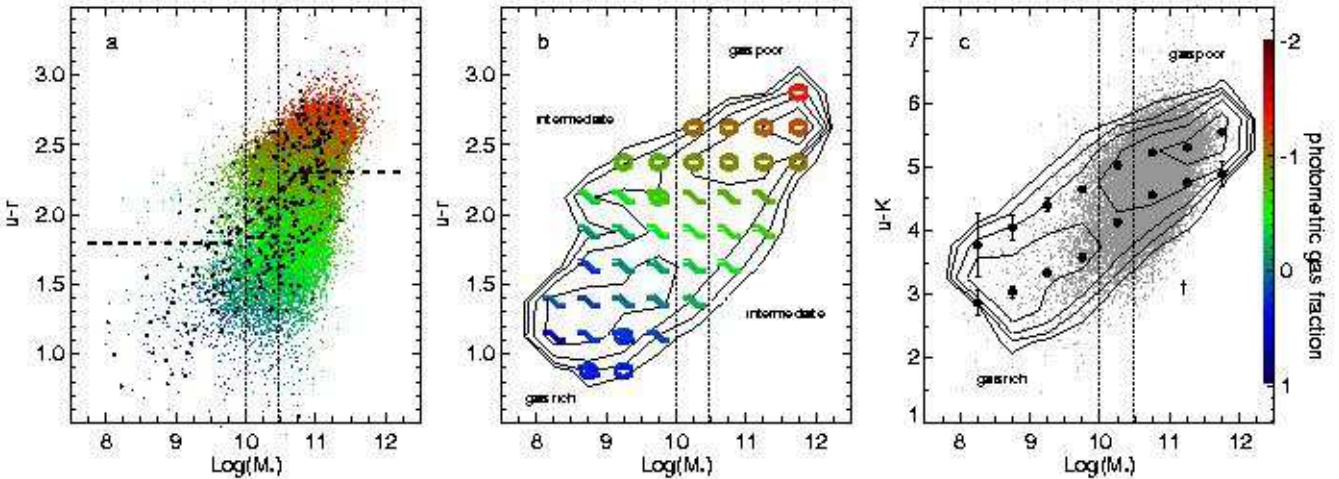


FIG. 2.— Color vs. the logarithm of stellar mass for the SDSS-2MASS sample. Vertical lines show the transition mass interval at  $1-3 \times 10^{10} M_\odot$ . (a) Individual  $u-r$  data points color-coded by photometric gas fractions (from  $u-K$  colors) as shown in Fig. 1c. The thick dashed line approximates the optimal  $u-r$  color division of the red and blue sequences from Baldry et al. (2004). Black dots mark galaxies used in the  $\mathrm{H}\alpha$  calibration (Figs. 1b and c). (b) Photometric gas fraction and morphology transitions within the red and blue sequences. Contours show the conditional probability distribution of  $u-r$  on  $M_*$ , in bins of  $0.25 \times 0.5$  in color  $\times \log(M_*)$ . Each galaxy is weighted by  $1/V_{\mathrm{max}}$  and all bins of a given mass are normalized by the total for that mass column. Symbols indicate the  $1/V_{\mathrm{max}}$ -weighted mean photometric gas fraction and concentration index  $C_r$  in each bin. Ovals and S-shaped marks bins with  $C_r > 2.55$  and  $C_r < 2.65$  to show early and late types, so transitional bins have both symbols. Each symbol has three colors to show the mean and  $\pm 1\sigma$  values of photometric gas fraction; an easy-to-see case is at  $(\log(M_*), u-r) \sim (11.8, 2.4)$ . (c) Photometric gas fractions and  $u-K$  colors vs. stellar mass. Contours give the conditional probability distribution of  $u-K$  on  $M_*$ , in bins of  $0.5 \times 0.5$  in color  $\times \log(M_*)$ . Large points show the weighted mean photometric gas fractions for the red and blue sequences separately, using the  $u-r$ -based division in panel a. The arrow estimates  $u-K$  evolution from the SDSS-2MASS sample redshift limit of  $z = 0.1$  to the median SDSS-2MASS-HYPERLEDA sample redshift of  $z = 0.017$ , averaging Bell et al. (2003) and Blanton et al. (2003c). All contours start at 0.04 and increase by  $10^{0.25} \times$  at each step.

tribution look qualitatively similar to the bimodal distribution of SFH vs. stellar mass reported by Kauffmann et al. (2003b).<sup>2</sup> This similarity suggests that the bimodality in SFHs may be intimately related to changes in gas-to-stellar mass ratios. The contours in Fig. 2c show a broad shift near  $\sim 10^{10} M_\odot$ , while the individual trends in the red and blue sequences change slope over the range  $\sim 1-3 \times 10^{10} M_\odot$  (though the latter changes are not independent of the method of separating the two sequences, based on the optimal color division of Baldry et al. 2004, shown in Fig. 2a). Kauffmann et al. also find a single-sequence bimodal structure in  $C_r$  vs.  $M_*$ , which is qualitatively consistent with the

decreased  $C_r$  seen in the low-mass red sequence in Fig. 2b.

Despite low concentrations and enhanced gas contents, the low-mass red sequence fits into the classic merger picture for the origin of early type galaxies. This sequence is clearly observed as an abundant population of faint, moderately gas-rich S0 and S0/a galaxies in the Nearby Field Galaxy Survey, a survey designed to represent the natural distribution of galaxy morphologies over a wide range of luminosities (Jansen et al. 2000; Kannappan et al. 2002, see Fig. 3 of the latter). Kannappan & Fabricant (2001) argue, based on the frequency of gas-stellar counterrotation in this population and the scarcity

<sup>2</sup> Note that the bimodalities in question are bimodalities in the conditional probability distribution and need not appear directly in the observed galaxy distribution.

of low-luminosity intermediate-type spiral galaxies, that  $\gtrsim 50\%$  of the low-luminosity S0 population may form via late-type dwarf mergers. Such gas-rich mergers will naturally produce remnants with modest concentration indices, explaining why low-luminosity early types are predominantly S0 rather than E galaxies. Furthermore, a large fraction of low-luminosity early types have blue, starbursting centers, despite red outer disks (Tully et al. 1996; Jansen et al. 2000), and many are also classified as blue compact dwarfs. Such blue-centered color gradients correlate with morphological evidence of mergers and interactions (in all morphological types, Kannappan et al. 2004). With these results in mind, it is likely that the SFH measures adopted by Kauffmann et al. (2003b), which are based on 3''-aperture spectroscopy, may emphasize the starbursting centers of this class of low-mass early-type systems (and conversely, the quiescent centers of high-mass late-type systems with red-centered color gradients), reinforcing the single-sequence structure of the resulting SFH vs. stellar mass plots.

#### 4. DISCUSSION

A connection between star formation histories and gas fractions is in some sense obvious: gas must be consumed to form stars, so old red stellar populations will tend to be associated with diminished gas supplies. However, galaxies also accrete and expel gas, so this simple view misses much of the story. A complete picture must explain why gas fractions depend on mass, and in particular why there is such a close coincidence between the transition to gas richness (G/S  $\sim 1:1$  in the blue sequence) and the shift to recent-burst dominated SFHs below  $M_*^t$ . Critical transition masses are predicted by scenarios involving starburst-driven gas blowout, inefficient star formation below a gravitational instability threshold, and/or cold-mode gas accretion (Dekel & Silk 1986; Verde et al. 2002; Birnboim & Dekel 2003; Katz et al. 2003; Dalcanton et al. 2004). Global gas blowout from recent-burst dominated SFHs cannot easily explain an *abundance* of gas in low-mass ( $10^8$ – $10^{10}$   $M_\odot$ ) galaxies, as found in this paper. However, localized gas blowout or strong feedback could inhibit efficient widespread star formation in low-mass disk galaxies. Such scenarios do not explicitly account for the gas in low-mass red-sequence galaxies, but late-type dwarf mergers, as discussed above, could allow these galaxies to acquire their modest gas excesses from gas-rich progenitors and thereby inherit a similar threshold mass for increased gas fractions. Alternatively, it is possible that the transition in star formation modes at  $\sim 2$ – $3 \times 10^{10}$   $M_\odot$  is not a

cause, but an *effect* of changing gas fractions, as in cold-mode accretion scenarios. If so, low-mass galaxies may form stars reasonably efficiently and still appear gas rich. The excess gas in low-mass red-sequence galaxies could in this case represent post-merger cold-mode accretion, possibly as part of a process of disk regrowth.

In conclusion, this paper has demonstrated a link between bimodal galaxy SFHs and a shift in gas richness at  $M_*^t \sim 1$ – $3 \times 10^{10}$   $M_\odot$ . The link may be causal in either direction, depending on the relative importance of supernova blowout, feedback, and cold-mode accretion processes in determining  $M_*^t$ . To establish this result, a technique has been introduced to estimate photometric gas fractions based on the correlation between  $u$ – $K$  colors and gas-to-stellar mass ratios. This correlation is interesting in its own right (see also Bothun 1984) and will be further examined and applied in future work.

I thank D. Mar for being a helpful sounding board and S. Faber for sparking my interest in galaxy bimodalities. N. Martinbeau and J. Huchra generously shared a catalog merging code for me to modify. I am also indebted to S. Jester, C. Gerardy, D. Mar, and P. Hoefflich for assistance with database and software issues. K. Gebhardt and R. Kennicutt provided useful comments on the original manuscript. This research has used the HYPERLEDA homogenized H $\alpha$  catalog (Vizier On-line Catalog VII/238). This work has also used data products from the Two Micron All Sky Survey, a joint project of the University of Massachusetts and the Infrared Processing and Analysis Center/California Institute of Technology, funded by the National Aeronautics and Space Administration (NASA) and the National Science Foundation (NSF). Funding for the Sloan Digital Sky Survey (SDSS) was provided by the Alfred P. Sloan Foundation, the Participating Institutions, NASA, the NSF, the U.S. Department of Energy, the Japanese Monbukagakusho, and the Max Planck Society. The SDSS is managed by the Astrophysical Research Consortium for the Participating Institutions, which are The University of Chicago, Fermilab, the Institute for Advanced Study, the Japan Participation Group, The Johns Hopkins University, Los Alamos National Laboratory, the Max-Planck-Institute for Astronomy, the Max-Planck-Institute for Astrophysics, New Mexico State University, the University of Pittsburgh, Princeton University, the United States Naval Observatory, and the University of Washington.

#### REFERENCES

Abazajian, K. et al. 2004, preprint (astro-ph/0403325)  
 Baldry, I. K., Glazebrook, K., Brinkmann, J., Ivezić, Ž., Lupton, R. H., Nichol, R. C., & Szalay, A. S. 2004, ApJ, 600, 681  
 Bell, E. F., McIntosh, D. H., Katz, N., & Weinberg, M. D. 2003, ApJS, 149, 289  
 Birnboim, Y. & Dekel, A. 2003, MNRAS, 345, 349  
 Blanton, M. R., et al. 2003a, AJ, 125, 2348  
 Blanton, M. R., et al. 2003b, ApJ, 594, 186  
 Blanton, M. R. et al. 2003c, ApJ, 592, 819  
 Boselli, A., Lequeux, J., & Gavazzi, G. 2002, A&A, 384, 33  
 Bothun, G. D. 1984, ApJ, 277, 532  
 Casoli, F., et al. 1998, A&A, 331, 451  
 Dalcanton, J. J., Yoachim, P., & Bernstein, R. A. 2004, preprint (astro-ph/0402472)  
 Dekel, A. & Silk, J. 1986, ApJ, 303, 39  
 Hogg, D. W., et al. 2002, AJ, 124, 646  
 Jansen, R. A., Franx, M., Fabricant, D., & Caldwell, N. 2000, ApJS, 126, 271  
 Jarrett, T. H., Chester, T., Cutri, R., Schneider, S., Skrutskie, M., & Huchra, J. P. 2000, AJ, 119, 2498  
 Kannappan, S. J. & Fabricant, D. G. 2001, AJ, 121, 140  
 Kannappan, S. J., Fabricant, D. G., & Franx, M. 2002, AJ, 123, 2358  
 Kannappan, S. J., Jansen, R. A., & Barton, E. J. 2004, AJ, 127, 1371  
 Katz, N., Keres, D., Dave, R., & Weinberg, D. H. 2003, in ASSL Vol. 281: The IGM/Galaxy Connection. The Distribution of Baryons at  $z=0$ , 185  
 Kauffmann, G., et al. 2003a, MNRAS, 341, 33  
 Kauffmann, G., et al. 2003b, MNRAS, 341, 54  
 Kennicutt, R. C. 1989, ApJ, 344, 685  
 Mac Low, M. & Ferrara, A. 1999, ApJ, 513, 142  
 Pérez-González, P. G., Gil de Paz, A., Zamorano, J., Gallego, J., Alonso-Herrero, A., & Aragón-Salamanca, A. 2003, MNRAS, 338, 525  
 Paturel, G., Theureau, G., Bottinelli, L., Gouguenheim, L., Coudreau-Durand, N., Hallet, N., & Petit, C. 2003, A&A, 412, 57  
 Roberts, M. S. 1969, AJ, 74, 859  
 Sanders, D. B. & Mirabel, I. F. 1996, ARA&A, 34, 749  
 Shaya, E. J. & Federman, S. R. 1987, ApJ, 319, 76  
 Strateva, I., et al. 2001, AJ, 122, 1861  
 Tully, R. B., Verheijen, M. A. W., Pierce, M. J., Huang, J., & Wainscoat, R. J. 1996, AJ, 112, 2471  
 Verde, L., Oh, S. P., & Jimenez, R. 2002, MNRAS, 336, 541